

Self-Assembling Nanocomposite Tectons

Jianyuan Zhang, Peter J. Santos, Paul A. Gabrys, Sangho Lee, Caroline Liu, and Robert J. Macfarlane*[ⓑ]

Department of Materials Science and Engineering, Massachusetts Institute of Technology, 77 Massachusetts Avenue, Cambridge, Massachusetts 02139, United States

S Supporting Information

ABSTRACT: The physical characteristics of composite materials are dictated by both the chemical composition and spatial configuration of each constituent phase. A major challenge in nanoparticle-based composites is developing methods to precisely dictate particle positions at the nanometer length scale, as this would allow complete control over nanocomposite structure–property relationships. In this work, we present a new class of building blocks called nanocomposite tectons (NCTs), which consist of inorganic nanoparticles grafted with a dense layer of polymer chains that terminate in molecular recognition units capable of programmed supramolecular bonding. By tuning various design factors, including the particle size and polymer length, we can use the supramolecular interactions between NCTs to controllably alter their assembly behavior, enabling the formation of well-ordered body-centered cubic superlattices consisting of inorganic nanoparticles surrounded by polymer chains. NCTs therefore present a modular platform that enables the construction of composite materials where the composition and three-dimensional arrangement of different constituents within the composite can be independently controlled.

Nanocomposites are an important class of materials based on integrating two or more disparate phases to achieve physical characteristics that cannot be realized with a single-phase material.^{1–4} The properties of these composites are dictated by their chemical compositions as well as the relative three-dimensional arrangements of each component. While structure control in macroscopic composites can be easily achieved via direct approaches such as mechanical processing, top-down methods to control nanoscale composite structure either provide limited spatial resolution or are undesirably inefficient. Alternatively, self-assembly can produce nanocomposite materials with well-defined geometries in a parallelizable manner that is amenable to scale-up. Indeed, many sophisticated nanoscale assembly techniques have been developed to synthesize materials with unique photonic, plasmonic, electronic, and mechanical properties,^{5–8} making use of multiple types of nanoscale building blocks, including polymers,^{9–11} biological materials,^{12,13} and inorganic nanocrystals.^{14–17} However, the major limitations of current nanocomposite self-assembly techniques are that they either (1) focus on ensuring compatibility of the different phases but lack hierarchical structural organization of all constituent components^{18–21} or (2) utilize directing agents or processing

conditions that are not amenable to functional composite architectures.^{22–24} In this work, we circumvented these challenges by developing a class of nanocomposite “tectons”^{25,26} (NCTs)—irreducible nanocomposite building blocks that are themselves composite materials (Figure 1). An NCT

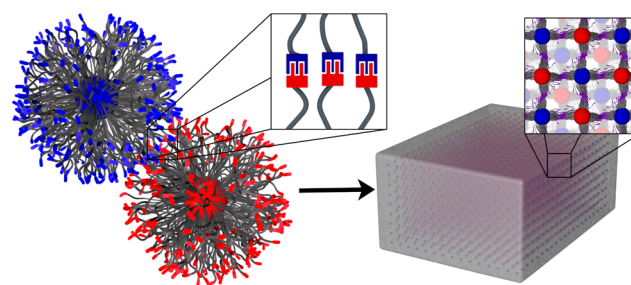


Figure 1. Nanocomposite tectons (left) use supramolecular binding interactions to form nanocomposite materials with spatial control over particle placement in three dimensions.

consists of a nanoparticle grafted with polymer chains that terminate in functional groups capable of supramolecular binding, where supramolecular interactions between polymers grafted to different particles enable programmable bonding that drives particle assembly (Figure 1). Importantly, these interactions can be manipulated separately from the structure of the organic or inorganic components of the NCT, allowing independent control over the chemical composition and spatial organization of all phases in the nanocomposite via a single design concept.

NCTs represent a versatile class of building blocks for nanocomposite synthesis, as the inorganic nanoparticle core provides a basic scaffold that dictates the size and shape of the NCT while the polymeric ligands define its solubility, the stiffness of its corona, and the interparticle distances in the final structure; together, these two components also dictate the overall chemical composition of the NCT. Conversely, the assembly process, and thus the final mesoscale ordering of particles within the composite, is dictated by the interactions between supramolecular binding groups. Indeed, the unique aspect of the NCT architecture is the use of these molecularly programmed interactions to enable more sophisticated control over particle assembly in the macroscopic composite than in previous polymer-grafted nanoparticle systems.

Here we demonstrate the first example of an NCT by grafting gold nanoparticles (AuNPs) with polystyrene (PS)

Received: October 23, 2016

Published: December 7, 2016

chains that terminate in molecular recognition units with complementary hydrogen-bonding motifs (diaminopyridine, DAP, and thymine, Thy). Gold nanoparticles provide a sensitive spectral probe for particle assembly²⁷ and are easily functionalized via gold–thiol chemistry, while PS can be synthesized with a wide range of molecular weights and low dispersity using controlled radical polymerization techniques such as atom transfer radical polymerization (ATRP).²⁸ Complementary hydrogen bonding²⁹ via the DAP and Thy units provides a simple means of controlling the particle interactions by modulating the temperature, as hydrogen bonds break upon addition of heat.

Functionalized PS polymers (DAP-PS and Thy-PS) were made from DAP- or Thy-modified initiators via ATRP, followed by postfunctionalization to install a thiol group that enabled particle attachment (Scheme S1). The polymers synthesized for the current study had three different molecular weights (~ 3.7 , ~ 6.0 , and ~ 11.0 kDa; Figure S1) with narrow dispersity ($\bar{D} < 1.10$) and were grafted to nanoparticles of different diameters (10, 15, 20, and 40 nm) via a “grafting-to” approach modified from a previous report.³⁰

Once synthesized, NCTs functionalized with either DAP-PS or Thy-PS were readily dispersed in common organic solvents such as tetrahydrofuran, chloroform, toluene, and *N,N'*-dimethylformamide and showed a typical plasmonic resonance extinction peak at 530–540 nm (Figures 2A and S2) that

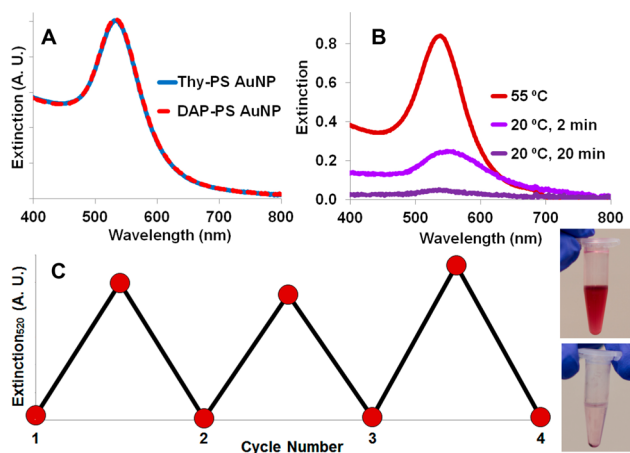


Figure 2. (A) Normalized UV–vis spectra of NCT dispersions in toluene (20 nm AuNPs, 11.0 kDa DAP-PS or Thy-PS). (B) UV–vis spectra of mixtures of complementary NCT dispersions. The three traces represent the spectrum 2 min after mixing, 20 min after mixing, and after heating at 55 °C for ~ 1 –2 min. (C) Normalized extinction at 520 nm for a mixture of complementary NCTs undergoing multiple heat–cool cycles between 20 and 55 °C (lower and upper data points, respectively; see the Supporting Information for details). Insets: optical images of a representative NCT mixture at the given temperatures.

confirmed their stability in these different solvents. Upon mixing, DAP-PS- and Thy-PS-coated particles rapidly assembled and precipitated from solution, resulting in noticeable red-shifting, diminishing, and broadening of the extinction peak within 1–2 min (an example with 20 nm AuNPs and 11.0 kDa polymers is shown in Figure 2B). Within 20 min, the dispersion appeared nearly colorless, and large purple aggregates had clearly precipitated from solution. After moderate heating (~ 55 °C for ~ 1 –2 min for the example in Figure 2B), the particles redispersed and the original color

intensity was regained, demonstrating the dynamicity and complete reversibility of the DAP–Thy directed assembly process. NCTs were taken through multiple heating and cooling cycles without any alteration of the assembly behavior or optical properties, signifying that they remained stable under each of these thermal conditions (Figure 2C).

A key feature of NCTs is that the sizes of their particle and polymer components can be easily modified independent of the supramolecular binding group’s molecular structure. However, because this assembly process is driven via the collective interaction of multiple DAP- and Thy-terminated polymer chains, alterations that affect the absolute number and relative density of DAP or Thy groups on the NCT surface impact the net thermodynamic stability of the assemblies. In other words, while all of the constructs should be thermally reversible, the temperature range over which particle assembly and disassembly occurs should be affected by these variables. To better understand how differences in NCT composition impact the assembly process, NCTs were synthesized using different nanoparticle core diameters (10–40 nm) and polymer spacer molecular weights (3.7–11.0 kDa) and allowed to fully assemble at room temperature (~ 22 °C). Particles were then monitored using UV–vis spectroscopy at 520 nm while slowly heating at a rate of 0.25 °C/min, resulting in a curve that clearly shows a characteristic disassembly temperature (melting temperature, T_m) for each NCT composition (Figure 3).

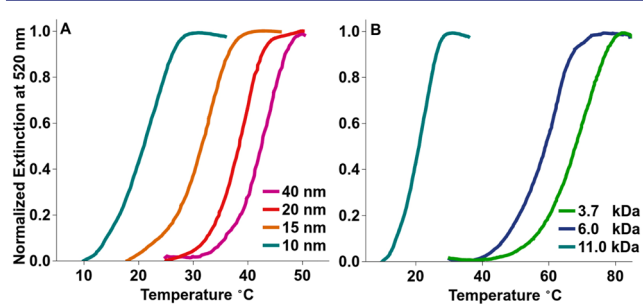


Figure 3. Thermal study of complementary NCT mixtures with (A) constant polymer molecular weight (11.0 kDa) and varying inorganic particle diameter or (B) constant particle diameter (10 nm) and varying polymer molecular weight.

From these data, two clear trends can be observed. First, when the polymer molecular weight is held constant, T_m increases with increasing particle size (Figure 3A). Conversely, when the particle diameter is kept constant, T_m drastically decreases with increasing polymer length (Figure 3B). To understand these trends, it is important to note that NCT melting is governed by a collective and dynamic dissociation of multiple individual DAP–Thy bonds that reside at the periphery of the polymer-grafted nanoparticles. The enthalpic component of NCT bonding behavior is therefore predominantly governed by the local concentrations of the supramolecular-bond-forming DAP and Thy groups, while the entropic component is dictated by differences in polymer configuration in the bound versus unbound states.

All of the NCTs in this study possess similar grafting densities (i.e., equivalent areal density of polymer chains at the inorganic nanoparticle surface; Figure S3) regardless of particle size or polymer length. However, the areal density of DAP and Thy groups at the periphery of the NCTs is not constant as a function of these two variables due to differences in NCT

geometry. When the inorganic particle diameter is increased, the decreased surface curvature of the larger particle core forces the polymer chains into a tighter packing configuration, resulting in an increased areal density of DAP and Thy groups at the NCT periphery,³¹ this increased concentration of binding groups therefore results in an increased T_m , explaining the trend in Figure 3A.^{32,33}

Conversely, for a fixed inorganic particle diameter (and thus constant number of polymer chains per particle), increasing the polymer length decreases the areal density of DAP and Thy groups at the NCT periphery as a result of a “splaying” of the polymers as they extend off the particle surface, thereby decreasing T_m in a manner consistent with the trend in Figure 3B. Additionally, increasing the polymer length results in a greater decrease in system entropy upon NCT assembly due to the greater reduction in the number of polymer configurations once the polymer chains are linked via a DAP–Thy bond; this would also be predicted to reduce T_m . While a more quantitative study of the melting behavior of NCTs is currently underway, we note that within the range tested, all of the samples were easily assembled and disassembled via alterations in temperature. The inorganic particle diameter and polymer length are therefore both effective handles to control the NCT assembly behavior.

Importantly, because the NCT assembly process is based on dynamic, reversible supramolecular binding, it should be possible to drive the system to an ordered equilibrium state where the maximum number of binding events can occur. We hypothesize that although the particle cores and polymer ligands are more polydisperse (Figure S1, S4 and Table S1) than the particles and small-molecule ligands used in prior studies to form nanoparticle superlattices,^{14,22} ordered arrangements still represent the thermodynamically favored state for a set of assembled NCTs. It is true that when NCTs are packed into an ordered lattice, deviations in particle diameter would be expected to generate inconsistent particle spacings that would decrease the overall stability of the assembled structure. However, the inherent flexibility of the polymer chains should allow the NCTs to adopt a conformation that compensates for these structural defects. As a result, an ordered NCT arrangement would still be predicted to be stable if it produced a larger number of DAP–Thy binding events than a disordered structure and this increase in binding events outweighed the entropic penalty arising from the reduction of polymer chain configurations once bound.

To test this hypothesis, multiple sets of assembled NCTs were thermally annealed at a temperature just below their T_m , allowing particles to reorganize via a series of binding and unbinding events (experimental details are provided in the Supporting Information) until they reached the thermodynamically most stable conformation. The resulting structures were analyzed with small-angle X-ray scattering (SAXS), which revealed the formation of highly ordered mesoscale structures in which the nanoparticles were arranged in body-centered cubic (bcc) superlattices (Figure 4, Figure S5, S6). The bcc structure was observed for multiple combinations of particle size and polymer length (Table S4), indicating that the nanoscopic structure of the composites can be controlled as a function of either the organic component (via the polymer length), the inorganic component (via the particle size), or both, making this NCT scheme a highly tailorable method for the design of future nanocomposites.

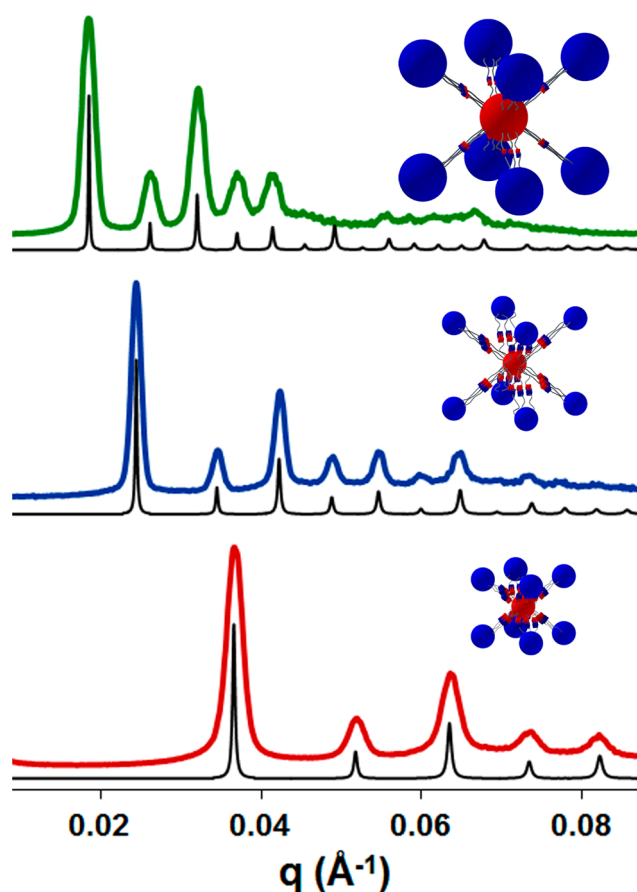


Figure 4. SAXS data showing NCT assembly into ordered bcc superlattices: (green trace) 20 nm AuNPs and 11.0 kDa PS; (blue trace) 10 nm AuNPs and 11.0 kDa PS; (red trace) 10 nm AuNPs and 6.0 kDa PS; (black traces) predicted SAXS patterns for the corresponding perfect bcc lattices. Insets: unit cells for the lattices drawn to scale.

In conclusion, we have demonstrated the versatility and programmability of NCTs as controllable nanocomposite building blocks. The data presented here provide the first example of this concept, and we predict that these NCTs should be amenable to multiple different particle core and polymer ligand formulations as well as different supramolecular binding motifs. Together, these design handles allow nanocomposite structure control at a level that is unrivaled by previous composite synthesis techniques. Future investigations will both explore the fundamental processes involved in NCT assembly and develop synthesis schemes for making solid and free-standing architectures from NCT building blocks. These structures are predicted to possess unique optical,³⁴ mechanical,³⁵ chemical,³⁶ and electrical properties⁵ that will make them highly desirable in multiple potential applications.

■ ASSOCIATED CONTENT

Supporting Information

The Supporting Information is available free of charge on the ACS Publications website at DOI: 10.1021/jacs.6b11052.

Detailed experimental procedure, characterization of the PS ligands, TGA data for the NCTs, and representative TEM images of the dried superlattice samples (PDF)

■ AUTHOR INFORMATION

Corresponding Author

*rmacfarl@mit.edu

ORCID 

Robert J. Macfarlane: 0000-0001-9449-2680

Notes

The authors declare no competing financial interest.

■ ACKNOWLEDGMENTS

This work was supported by the AFOSR (Award FA9550-11-1-0275) and made use of the MRSEC Shared Experimental Facilities at MIT, supported by the NSF under Award DMR-1419807. P.J.S. acknowledges support by the NSF Graduate Research Fellowship Program under Grant 1122374. S.L. acknowledges support from a scholarship from the Kwanjeong Education Foundation under Award 14AmB14D.

■ REFERENCES

- (1) Balazs, A. C.; Emrick, T.; Russell, T. P. *Science* **2006**, *314*, 1107.
- (2) Kumar, S. K.; Jouault, N.; Benicewicz, B.; Neely, T. *Macromolecules* **2013**, *46*, 3199.
- (3) Kango, S.; Kalia, S.; Celli, A.; Njuguna, J.; Habibi, Y.; Kumar, R. *Prog. Polym. Sci.* **2013**, *38*, 1232.
- (4) Kim, C. R.; Uemura, T.; Kitagawa, S. *Chem. Soc. Rev.* **2016**, *45*, 3828.
- (5) Talapin, D. V.; Lee, J.-S.; Kovalenko, M. V.; Shevchenko, E. V. *Chem. Rev.* **2010**, *110*, 389.
- (6) Rybtchinski, B. *ACS Nano* **2011**, *5*, 6791.
- (7) Boles, M. A.; Engel, M.; Talapin, D. V. *Chem. Rev.* **2016**, *116*, 11220.
- (8) Ghosh, S.; Maiyalagan, T.; Basu, R. N. *Nanoscale* **2016**, *8*, 6921.
- (9) Tang, C. B.; Lennon, E. M.; Fredrickson, G. H.; Kramer, E. J.; Hawker, C. J. *Science* **2008**, *322*, 429.
- (10) Bates, C. M.; Seshimo, T.; Maher, M. J.; Durand, W. J.; Cushen, J. D.; Dean, L. M.; Blachut, G.; Ellison, C. J.; Willson, C. G. *Science* **2012**, *338*, 775.
- (11) Sing, C. E.; Zwanikken, J. W.; Olvera de la Cruz, M. *Nat. Mater.* **2014**, *13*, 694.
- (12) Adler-Abramovich, L.; Gazit, E. *Chem. Soc. Rev.* **2014**, *43*, 6881.
- (13) Jones, M. R.; Seeman, N. C.; Mirkin, C. A. *Science* **2015**, *347*, 1260901.
- (14) Shevchenko, E. V.; Talapin, D. V.; Kotov, N. A.; O'Brien, S.; Murray, C. B. *Nature* **2006**, *439*, 55.
- (15) Talapin, D. V.; Nelson, J. H.; Shevchenko, E. V.; Aloni, S.; Sadtler, B.; Alivisatos, A. P. *Nano Lett.* **2007**, *7*, 2951.
- (16) Yan, W.; Xu, L.; Xu, C.; Ma, W.; Kuang, H.; Wang, L.; Kotov, N. A. *J. Am. Chem. Soc.* **2012**, *134*, 15114.
- (17) Paik, T.; Diroll, B. T.; Kagan, C. R.; Murray, C. B. *J. Am. Chem. Soc.* **2015**, *137*, 6662.
- (18) Zhao, Y.; Thorkeelsson, K.; Mastroianni, A. J.; Schilling, T.; Luther, J. M.; Rancatore, B. J.; Matsunaga, K.; Jinnai, H.; Wu, Y.; Poulsen, D.; Frechet, J. M. J.; Alivisatos, A. P.; Xu, T. *Nat. Mater.* **2009**, *8*, 979.
- (19) Heo, K.; Miesch, C.; Emrick, T.; Hayward, R. C. *Nano Lett.* **2013**, *13*, 5297.
- (20) Hashemi, A.; Jouault, N.; Williams, G. A.; Zhao, D.; Cheng, K. J.; Kysar, J. W.; Guan, Z. B.; Kumar, S. K. *Nano Lett.* **2015**, *15*, 5465.
- (21) Williams, G. A.; Ishige, R.; Cromwell, O. R.; Chung, J.; Takahara, A.; Guan, Z. B. *Adv. Mater.* **2015**, *27*, 3934.
- (22) Macfarlane, R. J.; Lee, B.; Jones, M. R.; Harris, N.; Schatz, G. C.; Mirkin, C. A. *Science* **2011**, *334*, 204.
- (23) Macfarlane, R. J.; O'Brien, M. N.; Petrosko, S. H.; Mirkin, C. A. *Angew. Chem., Int. Ed.* **2013**, *52*, 5688.
- (24) Ye, X.; Zhu, C.; Ercius, P.; Raja, S. N.; He, B.; Jones, M. R.; Hauwiler, M. R.; Liu, Y.; Xu, T.; Alivisatos, A. P. *Nat. Commun.* **2015**, *6*, 10052.
- (25) Wang, X.; Simard, M.; Wuest, J. D. *J. Am. Chem. Soc.* **1994**, *116*, 12119.
- (26) Hosseini, M. W. *Acc. Chem. Res.* **2005**, *38*, 313.
- (27) Storhoff, J. J.; Lazarides, A. A.; Mucic, R. C.; Mirkin, C. A.; Letsinger, R. L.; Schatz, G. C. *J. Am. Chem. Soc.* **2000**, *122*, 4640.
- (28) Matyjaszewski, K. *Macromolecules* **2012**, *45*, 4015.
- (29) Bertrand, A.; Lortie, F.; Bernard, J. *Macromol. Rapid Commun.* **2012**, *33*, 2062.
- (30) Goulet, P. J. G.; Bourret, G. R.; Lennox, R. B. *Langmuir* **2012**, *28*, 2909.
- (31) Jones, M. R.; Macfarlane, R. M.; Lee, B.; Zhang, J.; Young, K. L.; Senesi, A. J.; Mirkin, C. A. *Nat. Mater.* **2010**, *9*, 913.
- (32) Macfarlane, R. J.; Jones, M. R.; Senesi, A. J.; Young, K. L.; Lee, B.; Wu, J.; Mirkin, C. A. *Angew. Chem., Int. Ed.* **2010**, *49*, 4589.
- (33) Li, T. I. N. G.; Sknepnek, R.; Olvera de la Cruz, M. *J. Am. Chem. Soc.* **2013**, *135*, 8535.
- (34) Beaulieu, M. R.; Hendricks, N. R.; Watkins, J. J. *ACS Photonics* **2014**, *1*, 799.
- (35) Crosby, A. J.; Lee, J. Y. *Polym. Rev.* **2007**, *47*, 217.
- (36) Hui, C. M.; Pietrasik, J.; Schmitt, M.; Mahoney, C.; Choi, J.; Bockstaller, M. R.; Matyjaszewski, K. *Chem. Mater.* **2014**, *26*, 745.